

1

Superfluidity and Phase Correlations of Driven
Dissipative CondensatesJ. Keeling^a, L. M. Sieberer^b, E. Altman^c, L. Chen^d, S. Diehl^{b,e}, J. Toner^f**Abstract**

We review recent results on the coherence and superfluidity of driven dissipative condensates, i.e., systems of weakly-interacting non-conserved Bosons, such as polariton condensates. The presence of driving and dissipation has dramatically different effects depending on dimensionality and anisotropy. In three dimensions, equilibrium behaviour is recovered at large scales for static correlations, while the dynamical behaviour is altered by the microscopic driving. In two dimensions, for an isotropic system, drive and dissipation destroy the algebraic order that would otherwise exist, however a sufficiently anisotropic system can still show algebraic phase correlations. We discuss the consequences of this behaviour for recent experiments measuring phase coherence, and outline potential measurements that might directly probe superfluidity.

1.1 Introduction

This chapter is dedicated to superfluidity, and its relation to Bose-Einstein condensation, a topic with a long history. Many reviews of the concepts of condensation and superfluidity in thermal equilibrium can be found, see

^a SUPA, School of Physics and Astronomy, University of St Andrews, St Andrews KY16 9SS UK

^b Institute for Theoretical Physics, University of Innsbruck, A-6020 Innsbruck, Austria

^c Department of Condensed Matter Physics, Weizmann Institute of Science, Rehovot 76100, Israel

^d College of Science, China University of Mining and Technology, Xuzhou, Jiangsu 221116, Peoples Republic of China

^e Institute of Theoretical Physics, TU Dresden, D-01062 Dresden, Germany

^f Department of Physics and Institute of Theoretical Science, University of Oregon, Eugene, Oregon 97403, USA

for example Refs. [1, 2, 3, 4]. The focus of this chapter is on how these concepts apply (or fail to apply) to driven dissipative condensates — systems of bosons with a finite lifetime, in which loss is balanced by continuous pumping. We focus entirely on the steady state of such systems, neglecting transient, time dependent behaviour.

Experimentally, the most studied example of a driven dissipative condensate has been microcavity polaritons (see Ref. [5] and chapters... of this book). However similar issues can arise in many other systems, most obviously photon condensates [6], magnon condensates [7] and potentially exciton condensates (although typical exciton lifetimes are much longer than for polaritons). Even experiments on cold atoms could be driven into a regime in which such physics occurs, when considering continuous loading of atoms balancing three-body losses [8] or atom laser setups [9, 10, 11].

Experiments on polaritons are two dimensional, and in two dimensions it is particularly important to clearly distinguish three concepts often erroneously treated as equivalent: superfluidity, condensation, and phase coherence. This is because no true Bose-Einstein condensate exists in a homogeneous two-dimensional system. Before addressing superfluidity and phase coherence in the steady state of a driven dissipative system, we review in section 1.2 the essential ideas of condensation, superfluidity and phase coherence for systems in thermal equilibrium. In section 1.3 we set up a generic microscopic model for weakly interacting driven dissipative Bose gases, and make precise the sense in which these systems are non-equilibrium. Section 1.4 reviews the connection of these driven dissipative systems to the Kardar-Parisi-Zhang equation, and explains the absence, for isotropic systems, of algebraic order at large distances based on this mapping. We also show that algebraic order is possible in the strongly anisotropic case. We frame this discussion in the context of current experiments, which have all been done in the weakly anisotropic regime. In section 1.5 we discuss the meaning of superfluidity in a driven, number non-conserving setup and discuss experimental probes. Section 1.6 gives a brief account of vortices in such open systems. Conclusions and challenges for future research are given in section 1.7.

1.2 Bose-Einstein condensation and superfluidity

Bose-Einstein condensation for a gas of weakly interacting Bosons is a phase transition associated with the appearance of off-diagonal long range order (ODLRO) [12]. This means that correlation functions such as $\langle \psi^\dagger(\mathbf{r})\psi(\mathbf{r}') \rangle$ remain non-zero even between distant points, $|\mathbf{r} - \mathbf{r}'| \rightarrow \infty$. These cor-

relations indicate the spontaneous symmetry breaking of the $U(1)$ phase of the condensate wavefunction, i.e. writing $\psi = \sqrt{\rho}e^{i\theta}$, ODLRO corresponds to the phase θ being correlated at distant points. In such a symmetry broken phase there is a “phase stiffness”, i.e. there is an energy cost, $E[\theta(\mathbf{r})] = (K_s/2) \int d^2\mathbf{r}(\nabla\theta)^2$ for phase twists of the condensate.

A gedanken experiment to determine this phase stiffness is to measure the change of energy as one imposes a phase twist between the boundaries of the system. Alternatively, since phase gradients correspond to currents, a more practical way to measure the phase stiffness is to apply a force that tries to drive a current, and observe the condensate’s response. The behaviour of a condensate in a rotating container illustrates the role of the phase stiffness very clearly [2, 13]. The condensate cannot be made to rotate except by creating quantised vortices, and these cost energy due to the phase stiffness. Thus, for slow rotation, the condensate fails to rotate. Similar behaviour can be seen in a ring trap, where the core of a vortex can be located outside the condensate. This is the Hess-Fairbank [14] effect, and is a defining property of a superfluid. i.e., when a condensate has non-zero phase stiffness, it becomes superfluid, as seen by its reduced response to rotation.

However, superfluidity is not equivalent to Bose-Einstein condensation; as discussed below, in two dimensions, Bose-Einstein condensation and ODLRO do not exist, yet superfluidity persists. It is therefore useful to be able to define superfluidity directly without reference to condensation. This can be done, by defining a superfluid density as the part of the system that fails to respond to slow rotations. This definition also clarifies another important point: except at zero temperature, a system will have both superfluid and normal components, as thermally excited quasiparticles can respond normally to rotations. To identify the superfluid density we must consider the response function $\chi_{ij}(\mathbf{q}, \omega)$, which relates the current $\langle \hat{j}_i(\mathbf{q}, \omega) \rangle$ to the force that induces it, $f_j(\mathbf{q}, \omega)$:

$$\langle \hat{j}_i(\mathbf{q}, \omega) \rangle = \chi_{ij}(\mathbf{q}, \omega) f_j(\mathbf{q}, \omega), \quad (1.1)$$

where i, j refer to Cartesian components. The operator \hat{j}_i appearing here is the standard particle current written in momentum space;

$$\hat{j}_i(\mathbf{q}) = \sum_{\mathbf{k}} \hat{\psi}_{\mathbf{k}+\mathbf{q}}^\dagger \gamma_i(2\mathbf{k} + \mathbf{q}) \hat{\psi}_{\mathbf{k}}, \quad \gamma_i(\mathbf{K}) = \frac{K_i}{2m}.$$

We consider systems in which this current is conserved, i.e. $\partial_t \rho + \nabla \cdot \mathbf{j} = 0$, where ρ is the particle density. According to Noether’s theorem, current conservation corresponds to the existence of a $U(1)$ phase symmetry in the Hamiltonian — this is the same symmetry which is spontaneously broken on

Bose-Einstein condensation. Considering static (i.e. $\omega = 0$) long-wavelength (i.e. $\mathbf{q} \rightarrow 0$) currents, the most general response function possible for an isotropic system is:

$$\chi_{ij}(\mathbf{q} \rightarrow 0, \omega = 0) = \chi_L \frac{q_i q_j}{q^2} + \chi_T \left(\delta_{ij} - \frac{q_i q_j}{q^2} \right). \quad (1.2)$$

These terms χ_L, χ_T describe the response to longitudinal and transverse forces, i.e. $\mathbf{f} \parallel \mathbf{q}$, which occurs for a potential force, and $\mathbf{f} \perp \mathbf{q}$, which occurs for rotational or magnetic forces. Current conservation can be shown to mean that $(q_i q_j / q^2) m \chi_{ij}(\mathbf{q}, \omega) = \rho(\mathbf{q}, \omega)$, where $\rho(\mathbf{q}, \omega)$ is the single particle Green's function, so that indeed χ_L is related to the total particle number. The transverse part of χ_{ij} describes the response to rotations; therefore superfluidity corresponds to a reduction of χ_T . In a non-superfluid, current is parallel to force, which means $\chi_T = \chi_L$. The superfluid fraction of a system is therefore given by $(\chi_L - \chi_T)/\chi_L$, and the normal fraction by χ_T/χ_L .

The above definition of superfluidity depends on the *equilibrium* effect that a system in true thermal equilibrium has a reduced response to rotational forces. This effect is conceptually distinct from the *metastable* persistent flow that can also be seen in a non-simply connected (e.g. annular) geometry [2]. Metastable persistent flow occurs if one first sets the fluid in motion by rotating the container while above the critical temperature, and then cools the fluid until it becomes superfluid. If the container then stops rotating the fluid remains in motion, as the lifetime for the current to decay is exponentially large.

It is also important to note that the superfluid density defined above is a static property of the system; if excited dynamically, it is always possible to create excitations out of the condensate. Because the elementary spectrum of an interacting Bose gas has a linearly dispersing Bogoliubov sound mode, this sound velocity c_s acts as a critical velocity [2, 13, 4]: for a defect moving at a lower velocity, no excitations can be created beyond the condensed component. However, at non-zero temperatures, thermally excited quasi-particles can respond to flow at any velocity, and a normal component will occur, as discussed above. In equilibrium there is a fundamental connection between the existence of a non-zero sound velocity and the presence of a non-zero superfluid fraction: as discussed by [15], the finite frequency response function $\chi_{ij}(\mathbf{q}, \omega)$ has the same poles as the single particle Green's function, and so the finite frequency generalisation of the superfluid part of Eq. (1.2) is $\chi_{ij}^{SF}(\mathbf{q}, \omega) = c_s^2 q_i q_j / (c_s^2 q^2 - \omega^2)$. The fact that this is finite at $\omega = 0, \mathbf{q} \rightarrow 0$ is thus connected to the form of the dispersion and the existence of a non-zero sound velocity.

1.2.1 Two dimensions

In two dimensions, the distinction between superfluidity and BEC becomes even more important, since an homogeneous two dimensional system is unable to show true long-range order due to the Mermin-Wagner theorem [16]. This can be seen by considering the correlation function $\langle \psi^\dagger(\mathbf{r})\psi(\mathbf{r}') \rangle \simeq \rho_0 \langle \exp[i(\theta(\mathbf{r}') - \theta(\mathbf{r}))] \rangle$. Even for a system with a non-zero phase stiffness, $E[\theta(\mathbf{r})] = (K_s/2) \int d^2\mathbf{r} (\nabla\theta)^2$, the vanishing energy cost of long wavelength phase twists leads to a thermal expectation which, at long distances, takes the form

$$\left\langle e^{i(\theta(\mathbf{r}') - \theta(\mathbf{r}))} \right\rangle \propto \exp(-\alpha_s \ln |\mathbf{r} - \mathbf{r}'|) \propto |\mathbf{r} - \mathbf{r}'|^{-\alpha_s}, \quad \alpha_s = \frac{k_B T}{2\pi K_s}, \quad (1.3)$$

which vanishes algebraically as $|\mathbf{r} - \mathbf{r}'| \rightarrow \infty$. Therefore, there is no ODLRO, and so no single mode is macroscopically occupied; i.e., there is no BEC. Nonetheless, superfluidity can survive, because the phase stiffness K_s implies a resistance to rotation of the low energy modes of the condensate. In fact, either by directly comparing the calculation of phase stiffness and superfluid density [15], or by calculating the current-current response function from the parametrisation and energy functional above [1, 13], one finds that the phase stiffness (and thus the power law decay) is directly related to the superfluid stiffness: specifically, $K_s = \rho_s/m^2$ where m is the quasiparticle mass.

In addition to the distinct nature of the low temperature phase in two dimensions, the transition to this phase is also unusual. As noted above, a superfluid can be made to rotate by creating quantised vortices, in which the phase winds by 2π around a point, and the density of the condensate vanishes at that point. As discussed by Kosterlitz and Thouless [17, 18] and Berezinskii [19], the transition out of the superfluid phase occurs through the proliferation of these vortices. The phase boundary can be found by a renormalisation group approach [18, 20, 21], which predicts that if $K_s < (2/\pi)k_B T$, vortices proliferate and correlations decay exponentially, whereas for $K_s > (2/\pi)k_B T$, vortices are irrelevant at large scales and correlations decay algebraically. As a result, the exponent for the algebraic decay, Eq. (1.3) takes the universal value $\alpha_s = 1/4$ at the phase boundary, and the superfluid density undergoes a universal jump [20].

1.3 Modelling driven dissipative condensates

A driven dissipative system is by definition one that is coupled to more than one environment, or is driven by a time dependent pumping field. One

can therefore no longer apply equilibrium concepts, such as minimising free energy, or the fluctuation-dissipation theorem. For a given system, such as a weakly interacting dilute Bose gas, there are many different types of driving and dissipation. Some of these conserve particle number; others do not. In this chapter we consider the latter case, motivated by systems such as microcavity polaritons (for a review see [5] and chapters XX of this book).

Microcavity polaritons are superpositions of excitons and photons, and the photon part can leak out through the mirrors. To reach a steady state this loss must be replenished by a compensating pump. Several models can be written to describe this, with varying descriptions of the reservoir that replenishes the condensate [22, 23, 24]. All such models lead to the same essential differences between the equilibrium and driven dissipative cases. We consider the model starting from the weakly interacting dilute Bose gas,

$$\hat{H} = \int d^d r \hat{\psi}^\dagger(r) \left(-\frac{\nabla^2}{2m} \right) \hat{\psi}(r) + \frac{U}{2} \hat{\psi}^\dagger(r) \hat{\psi}^\dagger(r) \hat{\psi}(r) \hat{\psi}(r),$$

and consider loss terms described by the quantum master equation

$$\partial_t \rho = -i[\hat{H}, \rho] + \int d^d r \left(\frac{\kappa}{2} \mathcal{L}[\hat{\psi}(r), \rho] + \frac{\gamma}{2} \mathcal{L}[\hat{\psi}^\dagger(r), \rho] + \frac{\Gamma}{4} \mathcal{L}[\hat{\psi}^2(r), \rho] \right), \quad (1.4)$$

where $\mathcal{L}[\hat{X}, \rho] = 2\hat{X}\rho\hat{X}^\dagger - [\hat{X}^\dagger\hat{X}, \rho]_+$ is the usual Lindblad operator. The terms in Eq. (1.4) describe single particle loss, single particle incoherent pump, and two-particle losses at rates κ , γ , and Γ , respectively.

1.3.1 Mean-field description & collective excitations

The role of the dissipative terms in Eq. (1.4) can be seen by considering the corresponding mean-field equation of motion, found by replacing $\langle \psi(\mathbf{r}) \rangle = \varphi(\mathbf{r})$, and decoupling all correlators. This gives:

$$i\partial_t \varphi = \left[-\frac{\nabla^2}{2m} + U|\varphi|^2 + \frac{i}{2} (\gamma - \kappa - \Gamma|\varphi|^2) \right] \varphi, \quad (1.5)$$

which is a modified Gross–Pitaevskii equation [25] (GPE) including dissipative terms describing particle gain and loss. The nonlinear term with coefficient Γ describes gain saturation, or feedback between the condensate and the reservoir, which prevents the particle density from diverging. For small fluctuations around the steady state, $\Gamma|\varphi_0|^2 = \gamma_{\text{net}} \equiv \gamma - \kappa$, one finds the fluctuations have a complex spectrum $\omega_{\mathbf{k}}$ of the form:

$$\omega_{\mathbf{k}} = -i \left(\frac{\gamma_{\text{net}}}{2} \right) \pm \sqrt{\xi_{\mathbf{k}}^2 - \left(\frac{\gamma_{\text{net}}}{2} \right)^2}, \quad \xi_{\mathbf{k}}^2 = \frac{k^2}{2m} \left(\frac{k^2}{2m} + 2U|\varphi_0|^2 \right). \quad (1.6)$$

The quantity $\xi_{\mathbf{k}}$ reduces to the equilibrium Bogoliubov excitation spectrum in the limit $\kappa, \gamma, \Gamma \rightarrow 0$. As discussed in Sec. 1.2, $\xi_{\mathbf{k}}$ has a linear dispersion, $\xi_{\mathbf{k}} \simeq c_s |\mathbf{k}|$ at low momentum, where $c_s^2 = U|\varphi_0|^2/m$. In contrast, $\omega_{\mathbf{k}}$ is diffusive at low momentum, $\omega_{\mathbf{k}} = -iDk^2$ with $D = c_s^2/\gamma_{\text{net}}$.

This modified dispersion would appear to mean that the critical velocity vanishes. Nonetheless, signatures of a non-vanishing critical velocity can survive in static correlation functions — albeit washed out by dissipation. To see this one may calculate theoretically the drag force on a defect immersed in a steady flow pattern around the defect potential $V_{\text{defect}}(\mathbf{r})$. The static drag force on the defect is given by [26] $\mathbf{F}_{\text{drag}} \propto \int d^d \mathbf{r} \rho(\mathbf{r}) \nabla V_{\text{defect}}(\mathbf{r})$. For a perfect superfluid below the critical velocity, the flow pattern is symmetric, so that the effects of pressure ahead of and behind the defect cancel: i.e. “d’Alembert’s paradox” occurs, that an irrotational flow produces no drag. The GPE, with $\rho(r) = |\varphi(r)|^2$ describes such a perfect superfluid, and would thus normally predict zero drag, however, if one calculates the drag using the complex GPE given above, a finite drag force exists at all velocities [27, 28]. There does however remain a marked threshold at $v = c_s$ above which the drag increases more rapidly with velocity. This behaviour is similar to an equilibrium superfluid at finite temperature, however calculating the finite temperature drag for an equilibrium superfluid requires including fluctuations beyond the mean-field theory.

The modified dispersion also has effects on the linear-response calculation of phase correlations [29, 30], however as discussed below, a more dramatic change arises because a linearised theory becomes inadequate in calculating correlations of the driven dissipative Bose gas in two dimensions.

1.3.2 Beyond mean-field description

In order to calculate correlations and response functions, the mean-field description is not sufficient. Various methods for dealing with driven dissipative systems such as Eq. (1.4) exist. We consider an approach starting from the Schwinger-Keldysh path integral (see Ref. [31] for an introduction), defined by the “partition sum”

$$\mathcal{Z} = \int \mathcal{D}(\psi_C, \psi_Q) e^{iS[\psi_C, \psi_Q]}, \quad (1.7)$$

where S is the Schwinger-Keldysh action written in terms of “classical” and “quantum” fields ψ_C, ψ_Q . For the model in Eq. (1.4) this takes the form:

$$S[\psi_C, \psi_Q] = \int dt d^d r \left\{ (\bar{\psi}_C \quad \bar{\psi}_Q) \begin{pmatrix} 0 & [D_0^A]^{-1} \\ [D_0^R]^{-1} & [D_0^{-1}]_K \end{pmatrix} \begin{pmatrix} \psi_C \\ \psi_Q \end{pmatrix} \right. \\ \left. - \left[\left(\frac{U}{2} + i \frac{\Gamma}{4} \right) ((\bar{\psi}_C^2 + \bar{\psi}_Q^2) \psi_C \psi_Q) + \text{c.c.} \right] + i \Gamma \bar{\psi}_C \psi_C \bar{\psi}_Q \psi_Q \right\}, \quad (1.8)$$

where the bare inverse retarded Green’s function is given by $[D_0^R]^{-1} = i\partial_t - [-\nabla^2/(2m) + i(\gamma - \kappa)/2]$ in time and real space domain, or $\omega - [\epsilon_k + i(\gamma - \kappa)/2]$ in the frequency and momentum domain. The inverse advanced Green’s function $[D_0^A]^{-1}$ is the complex conjugate of this, and the Keldysh component of the inverse bare Green’s function $[D_0^{-1}]_K = i(\kappa + \gamma)$ describes the noise associated with both pumping and decay. Despite the existence of terms which create and destroy particles, Eq. (1.8) still possesses a $U(1)$ symmetry under simultaneous phase rotations of the fields ψ_C, ψ_Q ; as such there still exists the possibility of spontaneous symmetry breaking, phase stiffness, and of superfluidity.

Equations (1.7, 1.8) are fully equivalent to the quantum master equation, Eq. (1.4), but written in a functional integral formulation. This formulation allows one to apply a wide range of techniques from quantum field theory. A first, rather generic simplification consists in taking the *semiclassical limit*, which can be justified by a power counting argument. This is strictly justified close to the condensation threshold, where $\gamma - \kappa \rightarrow 0$, but provides a useful approximation also away from this limit. At threshold, the retarded and advanced inverse Green’s functions scale as $\sim k^2$ with $\omega \sim k^2$, while there is no scaling of the Keldysh component, $[D_0^{-1}]_K = i(\kappa + \gamma) \sim k^0$. Using these, along with the natural scaling $dr \sim k^{-1}, dt \sim \omega^{-1}$, we can then determine the scaling dimensions of the fields $\psi_C \sim k^{(d-2)/2}, \psi_Q \sim k^{(d+2)/2}$ required in order that the quadratic contributions to the action are dimensionless. This then allows determination of the scaling of the various quartic terms. Due to this scaling, any quartic term involving more than a single quantum field is irrelevant — i.e. such terms scale to zero at long wavelength $k \rightarrow 0$, and can thus be omitted in the semiclassical limit. This provides direct contact to the dissipative GPE (1.5). The field equation obtained from the saddle point, $\delta S / \delta \bar{\psi}_Q = 0$, of Eq. (1.8) in the semiclassical limit reads

$$i\partial_t \psi_C = \left[-\frac{\nabla^2}{2m} + \frac{U}{2} |\psi_C|^2 + \frac{i}{2} \left(\gamma - \kappa - \frac{\Gamma}{2} |\psi_C|^2 \right) \right] \psi_C + i(\kappa + \gamma) \psi_Q. \quad (1.9)$$

This almost matches Eq. (1.5) if one identifies $\varphi = \psi_C / \sqrt{2}$, but with an extra term involving the quantum field ψ_Q .

While the “classical” field can acquire a finite expectation in the condensed state, the “quantum” field has to vanish on average and describes the noise. As a saddle point equation, Eq. (1.9) neglects the fluctuations of the fields ψ_C, ψ_Q , appearing in the full functional integral. Remarkably, this equation can be upgraded to a full description of the problem by means of the Martin-Siggia-Rose construction [31]. This shows that the functional integral Eq. (1.7) in the semiclassical limit is *equivalent* to a stochastic partial differential equation. In our case, this is the driven dissipative stochastic Gross-Pitaevskii equation (DSGPE) which is equivalent to Eq. (1.9) with the replacement $i(\kappa + \gamma)\psi_Q \rightarrow \xi(\mathbf{r}, t)$, where $\xi(\mathbf{r}, t)$ describes a Gaussian white noise process characterised by $\langle \xi(\mathbf{r}, t) \rangle = 0$ and $\langle \xi(\mathbf{r}, t) \bar{\xi}(\mathbf{r}', t') \rangle = \frac{\gamma + \kappa}{2} \delta(t - t') \delta(\mathbf{r} - \mathbf{r}')$, and vanishing off-diagonal correlators. In this sense, the DSGPE corresponds to a fully fluctuating (semiclassical) many-body problem — in stark contrast to the deterministic GPE (1.5).

1.3.3 Equilibrium vs. non-equilibrium dynamics

The action (1.8) in the semiclassical limit or the DSGPE allow us to state precisely the sense in which the driven dissipative system is a genuinely non-equilibrium situation. To this end we rewrite Eq. (1.9) by splitting the deterministic parts on the RHS into coherent (reversible) and dissipative (irreversible) contributions labelled c, d . To avoid confusion with these labels we omit the suffix C on the classical field ψ_C . The DSGPE takes the form:

$$i\partial_t \psi = \frac{\delta H_c}{\delta \bar{\psi}} - i \frac{\delta H_d}{\delta \bar{\psi}} + \xi \quad (1.10)$$

with effective coherent and dissipative Hamiltonians

$$H_{\alpha=c,d} = \int d^d r \left(K_\alpha |\nabla \psi|^2 + r_\alpha |\psi|^2 + \frac{u_\alpha}{2} |\psi|^4 \right). \quad (1.11)$$

The coefficients are $K_c = 1/2m, K_d = 0, r_c = 0, r_d = (\gamma - \kappa)/2, u_c = U/2$ in our problem, and $u_d = \Gamma/4$. Note, however, that the value of r_c is adjustable by a gauge transformation $\psi \mapsto \psi e^{-i\omega t}$ such that $r_c \mapsto r_c - \omega$. It can be shown [32, 33] that if the system is to relax to thermodynamic equilibrium (if the steady state of Eq. (1.10) is to be described by a Gibbs distribution), then the coherent and dissipative Hamiltonians must be proportional to each other; that is,

$$H_c = \nu H_d \quad \Leftrightarrow \quad \nu = \frac{K_c}{K_d} = \frac{u_c}{u_d} \quad (1.12)$$

where ν is a constant.

This requirement is in general not satisfied for a driven dissipative system because the microscopic origins of reversible and irreversible dynamics are independent. For example, in the microscopic description of Eq. (1.4) the rates can be tuned independently from the Hamiltonian parameters, as they have completely different physical origins.

We have thus far made two important observations pertaining to a driven condensate. One is that, in spite of particle number non-conservation, the equations of motion describing an incoherently driven condensate enjoy a $U(1)$ phase symmetry. The second observation is that the steady state cannot be in general described by an equilibrium ensemble. So, while a condensation transition involving spontaneous symmetry breaking is possible, the nature of the transition and the conditions under-which such a condensate would be indeed a stable fixed point of the dynamics may be different from the equilibrium case.

The question concerning the nature of the condensation transition in three dimensional driven condensates was addressed in Refs. [34, 33, 35]. One main result of this analysis was that the equilibrium symmetry, $H_c = \nu H_d$ is emergent in the low frequency limit even though it is not present microscopically. Hence the *correlation* functions correspond to an effective equilibrium description with a well defined emergent temperature. Nevertheless, the drive conditions affect the long wavelength dynamical *response* functions, guaranteed by the existence of a new and independent critical exponent.

In two dimensions, as we will show next, the long wavelength behaviour is changed much more dramatically: in isotropic systems, the slow algebraic decay of correlation functions that occurs in equilibrium is replaced by far faster exponential or stretched exponential decay. Only for sufficiently anisotropic systems can the quasi-long-ranged algebraic decay found in equilibrium be recovered.

1.4 Long wavelength fluctuations and phase coherence

As discussed in Sec. 1.2, the Mermin-Wagner theorem states that a homogeneous equilibrium system with a continuous symmetry cannot show long-range order that breaks that continuous symmetry in two or fewer dimensions. Rather, in two dimensions, long-wavelength phase fluctuations lead to algebraic decay of order parameter correlations. Naturally the question arises whether this statement remains true out of equilibrium. The answer to this question proves to depend on both dimensionality, and anisotropy. In three dimensions, the deviation from effective equilibrium, which is encoded

in the difference between the ratios K_c/K_d and u_c/u_d (cf. Eq. (1.12)), vanishes in the long-wavelength limit, both close to criticality [34], and in the ordered (Bose condensed) phase [36]. However, in isotropic two dimensional systems, these non-equilibrium effects are relevant [36], and ultimately lead to the destruction of algebraic order. There is, however, a loophole: a spatially *anisotropic* system can support an algebraically ordered phase. These conclusions follow from a hydrodynamic description of the order parameter dynamics, which we review in the following.

In order to allow for spatial anisotropy, we consider a generalisation of the model described by Eq. (1.10), in which the gradient terms in the effective Hamiltonians (1.11) are replaced by $\sum_{i=x,y} K_\alpha^i |\partial_i \psi|^2$. As described in Sec. 1.2, a hydrodynamic description can be obtained by employing a density-phase representation, $\psi = \sqrt{\rho} e^{i\theta}$, leading to coupled equations of motion for the density ρ and phase θ . Eliminating the gapped fluctuations of the density around its mean value ρ_0 , and keeping only the leading terms in a low-frequency and low-momentum expansion in the remaining equation for the phase, we obtain the anisotropic Kardar-Parisi-Zhang [37] (KPZ) equation [36],

$$\partial_t \theta = \sum_{i=x,y} \left[D_i \partial_i^2 \theta + \frac{\lambda_i}{2} (\partial_i \theta)^2 \right] + \eta, \quad (1.13)$$

where $\eta(\mathbf{r}, t)$ is a Gaussian stochastic noise with zero mean, $\langle \eta(\mathbf{r}, t) \rangle = 0$, and second moment $\langle \eta(\mathbf{r}, t) \eta(\mathbf{r}', t') \rangle = 2\Delta \delta(\mathbf{r} - \mathbf{r}') \delta(t - t')$, with

$$\Delta = \frac{(\kappa + \gamma) (u_c^2 + u_d^2)}{2u_d (\kappa - \gamma)}. \quad (1.14)$$

The effective diffusion constants in Eq. (1.13) and the non-linear couplings are given by

$$D_i = K_c^i \left(\frac{K_d^i}{K_c^i} + \frac{u_c}{u_d} \right), \quad \lambda_i = -2K_d^i \left(\frac{K_c^i}{K_d^i} - \frac{u_c}{u_d} \right). \quad (1.15)$$

Evidently the non-linear terms in the KPZ equation vanish when the equilibrium condition $K_c^x/K_d^x = K_c^y/K_d^y = u_c/u_d$, which generalises Eq. (1.12) to the spatially anisotropic case, is met. The degree of anisotropy is measured by the anisotropy parameter $\Phi = \lambda_y D_x / \lambda_x D_y$: when $\Phi \neq 1$, the system is anisotropic.

An important difference exists between our KPZ model and the original context of this equation, as an equation for the interface height in a model of randomly growing interfaces [37]. The analogue of the interface height in our model is actually a phase, θ , and the phase is compact, i.e. $\theta \equiv$

$\theta + 2\pi$. This means that topological defects in this field — vortices — are possible. This difference with the conventional KPZ equation also arises in “Active Smectics” [38]. Analysis of Eq. (1.13) in the absence of vortices is the analogue of the low temperature spin-wave (linear phase fluctuation) theory of the equilibrium XY model. Indeed, without the non-linear terms, the KPZ equation reduces to linear diffusion, which would bring the field to an effective thermal equilibrium with power-law off-diagonal correlations (in $d = 2$). A transition to the disordered phase in this equilibrium situation can occur only as a Kosterlitz-Thouless (KT) transition through proliferation of topological defects in the phase field.

Our aim is to obtain the behaviour of correlations of the condensate field ψ at large distances. We have taken the first step of reducing this task to finding the correlations of the phase field θ , whose dynamics are given by the KPZ equation (1.13). But this equation contains more information than is actually required: in particular, it involves fluctuations with all wavelengths, ranging from the microscopic condensate healing length ξ_0 up to the largest scales of order of the linear system size L (we consider a square 2D system of area L^2). Because of the nonlinear term, fluctuations at different wavelengths couple to each other. Our goal, therefore, is to eliminate the short scale fluctuations, and in this way obtain an effective description of the system at large scales.

This idea is implemented by the renormalisation group procedure [21]. To this end, we decompose the phase field into short- and long-wavelength components, above and below some length scale ℓ . We then integrate out the short-wavelength components, treating the nonlinear terms $\lambda_{x,y}$ which couple short- and long-wavelength components perturbatively. As such this approach is limited to close-to-equilibrium conditions in which the couplings $\lambda_{x,y}$ are small¹. This procedure is then iterated for increasing lengthscales ℓ , successively integrating out the short wavelength components. In real space this corresponds to repeated coarse-graining, eliminating fine details on scales shorter than ℓ . Performing this program for the anisotropic KPZ equation [39, 38], the resulting equation for the long-scale components of the phase field again takes the form (1.13), but with coefficients that are modified by the short-scale fluctuations.

The modification of the coefficients as one goes to long length scales can be characterised entirely by the “flow” of two dimensionless parameters: These are a dimensionless form of the non-linearity, $g \equiv \lambda_x^2 \Delta / D_x^2 \sqrt{D_x D_y}$ and the anisotropy parameter $\Phi = \lambda_y D_x / \lambda_x D_y$ introduced below Eq. (1.15). The parameter g describes the importance of the nonlinear terms λ_x , for “typical” (i.e. root mean squared) fluctuations of the field θ . The mean squared

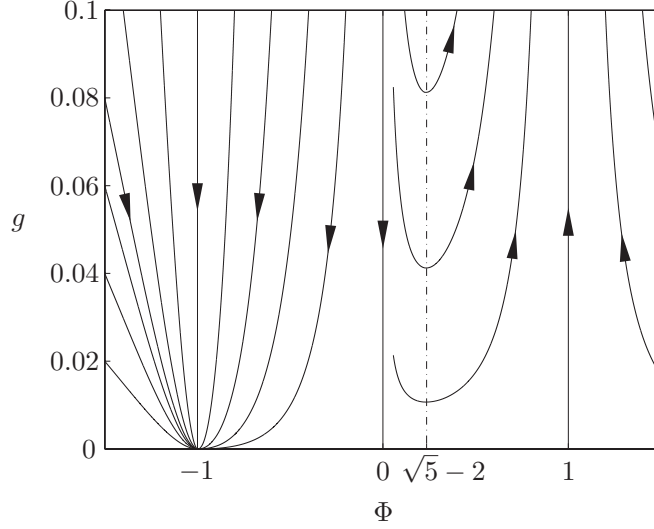


Figure 1.1 RG flow for the anisotropic KPZ equation in 2D. In the weakly anisotropic regime $\Phi > 0$, the flow lines approach the isotropic line $\Phi = 1$ and flow towards $g \rightarrow \infty$; for $\Phi < 0$, in the strongly anisotropic regime, they converge to a stable effective equilibrium fixed point with $\Phi = -1$ and $g = 0$.

fluctuations of θ , according to the linear theory, are proportional to the noise strength Δ , which drives the fluctuations, and inversely proportional to the geometric mean of the diffusion coefficients $D_{x,y}$, which smooth out those fluctuations. Knowing the anisotropy parameter Φ , together with g , then allows us to estimate the importance of the other non-linearity λ_y . The microscopic parameters of the system determine the “bare” values g_0 and Φ_0 at the starting length scale $\ell = \xi_0$. The values of g, Φ at some other scale $\ell > \xi_0$ are obtained by integrating the RG flow equations

$$\begin{aligned} \frac{dg}{dl} &= \frac{g^2}{32\pi} (\Phi^2 + 4\Phi - 1), \\ \frac{d\Phi}{dl} &= \frac{\Phi g}{32\pi} (1 - \Phi^2), \end{aligned} \quad (1.16)$$

with the logarithmic scale $l = \ln(\ell/L)$. The resulting RG flow is illustrated in Fig. 1.1. There are two distinct flow patterns to the left and right of the line $\Phi = 0$ and we discuss these in turn.

For $\Phi > 0$ the flow with increasing ℓ is towards strong coupling, $g \rightarrow \infty$, and isotropy, $\Phi \rightarrow 1$. Thus, in this regime, which we denote *weak anisotropy*, the approximation of treating g perturbatively eventually fails. Simulations of the isotropic KPZ equation [40, 41, 42, 43, 44, 45] find that correlations

of the phase field $\langle(\theta(\mathbf{r}) - \theta(\mathbf{r}'))^2\rangle$ scale algebraically with separation $|\mathbf{r} - \mathbf{r}'|$. This suggests that ultimately the flow of g must terminate at a strong coupling fixed point g_* , which is however beyond the scope of the perturbatively derived flow equations (1.16). This scaling of $\langle(\theta(\mathbf{r}) - \theta(\mathbf{r}'))^2\rangle$ would lead, according to Eq. (1.3) to stretched exponential decay of condensate field correlations.

Note, however, that in our analysis of the KPZ equation (1.13) we have so far neglected topological defects, which can exist in the compact field θ . Proliferation of such defects at the strong coupling fixed point would lead to exponential (i.e., even faster) decay of correlations of ψ .

The regime of *strong anisotropy*, on the other hand, corresponds to the region $\Phi < 0$. There the flow lines terminate for $\ell \rightarrow \infty$ in an effective *equilibrium* fixed point with $g = 0$ and $\Phi = -1$. Thus, in this regime, the effective description of the system at large scales approaches the equilibrium description (note that $g \propto \lambda_x^2$ and hence $g = 0$ in equilibrium), and so algebraic correlations of the condensate field can survive (as long as one is below the KT transition temperature).

The possibility of a flow to strong coupling is in stark contrast to the 3D case in which even in isotropic systems with $\Phi = 1$ small deviations $g \ll 1$ from equilibrium are irrelevant and flow to zero as $\ell \rightarrow \infty$, leading to the effective equilibrium physics discussed at the end of Sec. 1.3.3. Note, however, that even in 3D, for sufficiently strong drive and dissipation, i.e., values of g larger than some critical value, there may be a non-equilibrium transition to the disordered phase, described by the strong coupling fixed point of the 3D KPZ equation [46]. In one dimension, even equilibrium systems show only short range (exponential) correlations at non-zero temperatures. Nonetheless, it is still possible to see the effect of the KPZ nonlinearity on the scaling of the spatial [47] and temporal coherence [48, 49] of a one dimensional condensate.

1.4.1 *Current experiments, weak anisotropy, BKT physics and crossovers*

As discussed in chapter 25 [Kim, Nitsche, Yamamoto], experiments on incoherently pumped polariton condensates [29, 50] have measured an apparent algebraic decay of correlations, by measuring the fringe visibility in an interference experiment. Similar results have also been seen in numerical experiments on a parametrically pumped (OPO) system [51]. Since, as discussed above, algebraic order is destroyed at large scales, a question arises about the interpretation of these experiments. In this section we discuss how, although

the asymptotic behaviour at $\ell \rightarrow \infty$ does lead to the strong coupling fixed point, the length scales ℓ required to see this may be very large, particularly when the condensate is well developed.

Current experiments with exciton-polaritons fall into the regime of weak anisotropy. This anisotropy results from the interplay between polarisation pinning to the crystal structure, and the splitting of transverse electric and transverse magnetic cavity modes [5, 52] — taken together these mean that there is anisotropy between directions parallel and perpendicular to this pinned lattice direction. As discussed above, for weak anisotropy, the flow is to strong coupling and algebraic order is absent on the largest scales. However at intermediate scales, $g(\ell) \ll 1$, and so correlations can still decay algebraically. It is therefore natural to ask how large the system must be to see the breakdown of algebraic correlations — i.e. what system size L is required such that $g(L) \simeq 1$. Setting $\Phi = 1$ in the flow equation for g in Eq. (1.16), we find that if the microscopic parameters in Eq. (1.11) correspond to close-to-equilibrium conditions, i.e., if the bare value $g_0 \ll 1$, then the renormalised value $g = 1$ is reached only at the exponentially large characteristic KPZ scale $L = L_* = \xi_0 \exp(8\pi/g_0)$. Starting from a microscopic model for polariton condensation [5] that models the excitonic reservoir explicitly, and which provides a more faithful description of the condensation dynamics than the model of Eq. (1.4), we obtain the expression for the bare non-linearity [36]

$$g_0 = \frac{2u_c \bar{\gamma}^2}{K_c} \frac{\bar{\gamma}^2 + (1+x)^2}{x(1+x)^3}, \quad (1.17)$$

which depends on the dimensionless net pumping rate $x = \gamma/\kappa - 1$, and the dimensionless combination $\bar{\gamma} = \kappa R/\gamma_R u_c$, where R and γ_R are the rate of scattering between the excitonic reservoir and condensate, and the reservoir relaxation rate, respectively. The dimensionless parameter x gives a measure of how far above “threshold” the system is pumped. For high pump rates the KPZ scale L_* grows rapidly beyond any reasonable system size, so that a sufficiently strongly pumped system will always appear algebraically ordered up to system size L . Such a system resides effectively in equilibrium, with a temperature set by the noise strength. The form of Eq. (1.17) implies that for *any* finite system size L , it is always possible to choose a value x large enough that algebraic correlations are seen over the entire system. As such, the experimental observation of algebraic correlations is perfectly consistent with the results here.

At weak pump rates, near the threshold $x \rightarrow 0$, the bare coupling g_0 grows and so the critical size L_* decreases, and may become comparable

to the system size L . This then prompts a second question: as the pump strength is reduced, does the algebraic order break down before the KT transition occurs? As long as $L_* \gg L$, the system is effectively thermal and consequently it can undergo a KT transition to a disordered phase as described in Sec. 1.2 if x is decreased below a critical value x_{KT} . One can then evaluate the length scale L_* at this pump rate, i.e. we denote $L' \equiv L_*(x = x_{KT}) \approx \xi_0 \exp(2/\bar{\gamma}^2)$. If the system is much smaller than this critical size (i.e., $L \ll L'$), then even at the KT point, $L \ll L_*$, and so the KPZ physics does not become apparent. This is consistent with recent experiments on exciton polaritons [50] which showed the behaviour expected of a KT transition as discussed in Sec. 1.2.1 — i.e. a transition between algebraic order with exponent $\alpha_s = 1/4$ right at the transition and short ranged, exponentially decaying order. Such behaviour is consistent with a system of size $L \ll L'$. However, if the system is sufficiently large [36], i.e., $L \gg L'$, then algebraic order at length scale L will break down before the KT transition. The dependence of L' on $\bar{\gamma}$ can be understood intuitively: as $\bar{\gamma} \rightarrow 0$, then the polariton lifetime diverges, and thermalisation is perfect for any finite size system. Therefore $L' \rightarrow \infty$ and strong coupling with $g \approx 1$ is never reached. Thus, in order to clearly see the breakdown of algebraic order, one should increase the polariton loss rate κ .

1.4.2 Strong anisotropy, re-entrant phase transition

While the above analysis shows that the algebraic order observed in recent experiments with (nearly) isotropic polariton systems (see chapter 25 [Kim, Nitsche, Yamamoto] and Refs. [29, 50]) must be an intermediate scale crossover phenomenon, true algebraic order in the thermodynamic limit is nevertheless possible in the *strong anisotropy* regime, $\Phi_0 < 0$ as discussed above. We discuss here the experimental consequences this would have for a sufficiently anisotropic polariton system.

The effective temperature of the system at the strong anisotropy fixed point is given by the *renormalised* value of the dimensionless noise $\tau \equiv \Delta/\sqrt{D_x D_y}$. Because the phase is a compact variable, algebraic order only exists if this effective noise temperature is low enough. Specifically the KT transition occurs if the renormalised value of this dimensionless noise reaches π . One may then derive a phase diagram by identifying the location of this condition $\tau(\ell \rightarrow \infty) = \pi$ in the manifold of *bare* couplings, i.e. in terms of the microscopic experimental parameters. To do this we must complement the RG flow equations (1.16) for g and Φ by additional equations for τ and $D_{x,y}$ (see Ref. [38] for details), and follow the flow to the effective equilibrium

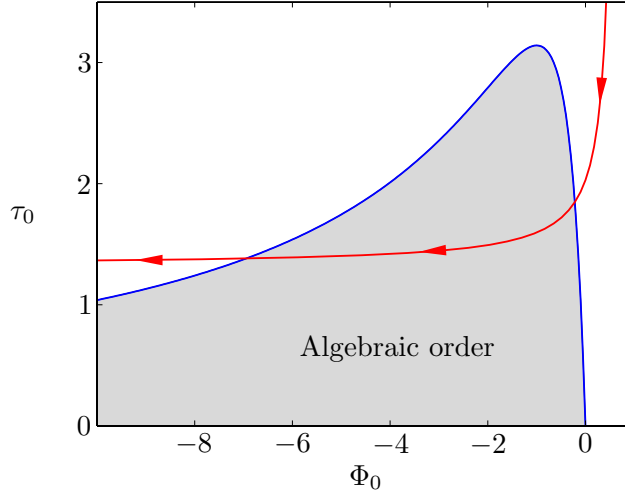


Figure 1.2 Phase diagram of a 2D anisotropic driven dissipative system for low noise. The thin line corresponds to values of Φ_0 and τ_0 derived from a microscopic model for polariton condensation [36], with the arrows indicating the direction of increasing pump rate γ . Note that the ordered phase is first entered and then left again as γ is increased. Values for the other dimensionless parameters are $\bar{\gamma} = 2$, $\bar{u} = 2$, $K_d^x/K_c^x = 1/8$, and $K_d^y/K_c^y = 1/4$.

regime $g \approx 0$. We must also assume that, up to the length scale at which the latter regime is reached, vortices are sufficiently dilute that their influence on the RG flows can be neglected. It turns out that the renormalised value τ of the dimensionless noise strength crosses the critical value for the KT transition for bare values τ_0 and Φ_0 that are located on the curve determined by

$$\tau_0 = -\frac{4\pi\Phi_0}{(1-\Phi_0)^2}. \quad (1.18)$$

The resulting phase diagram of strongly anisotropic driven dissipative systems in the $\Phi_0 - \tau_0$ plane is depicted in Fig. 1.2.

It is interesting to work out the bare parameters Φ_0 and τ_0 starting from the same microscopic model for polariton condensation that led to the estimate of g_0 in Eq. (1.17). This leads to a particular trajectory through the $\Phi_0 - \tau_0$ phase diagram as one increases the microscopic pump rate γ ; this trajectory is shown on Fig. 1.2. An initially moderate anisotropy, i.e., $\Phi_0 > 0$ but different from 1, becomes more substantial as the pump rate is increased, so that Φ_0 first becomes negative and then, if the value of the dimensionless interaction strength $\bar{u} = u_c/\sqrt{K_c^x K_c^y}$ is sufficiently small

(for details see Ref. [36]), crosses the boundary to the algebraically ordered phase. Remarkably, upon pumping the system at an even higher rate the ordered phase is then left again; that is, the transition is *reentrant*.

1.5 How to define and measure superfluidity in a dissipative system

In the previous section we have discussed how the presence of drive and dissipation affect the low energy effective theory of the two-dimensional system, and how these changes are manifested in the correlation functions of the system. In this section, we focus instead on the current-current response function, $\chi_{ij}(\mathbf{q}, \omega)$ for a dissipative system, and how to identify whether a superfluid fraction survives. The discussion in this section is focused on the case where phase fluctuations remain small, i.e. when the nonlinear term in the KPZ equation does not dominate the physics. As discussed above, this requires either a small finite system (as in the current experiments), or a system with sufficiently anisotropic interactions. While the calculations presented below can easily be extended to the anisotropic case, we present results only for the isotropic situation. When the nonlinearity in the KPZ equation becomes large, and algebraic correlations are destroyed, there may still exist a finite superfluid fraction; for a discussion of this point see [53]. However, if the growth of the KPZ nonlinearity ultimately leads to vortex proliferation and short range order, no superfluid fraction is expected to survive in the thermodynamic limit.

The response function $\chi_{ij}(\mathbf{q}, \omega = 0)$ for a non-equilibrium system can be calculated by defining a generating functional for correlations of currents. As noted in section 1.3.2, the driven dissipative system no longer has a conserved current, but does still show a $U(1)$ phase symmetry.

How then does the system respond to a phase twist between the boundaries of the system [54]? Such a physical phase twist couples to the unphysical “quantum” current $j_{Q,i}(\mathbf{q}) = \sum_{\mathbf{k}} [\bar{\psi}_{C,\mathbf{k}+\mathbf{q}} \psi_{Q,\mathbf{k}} + \bar{\psi}_{Q,\mathbf{k}+\mathbf{q}} \psi_{C,\mathbf{k}}] \gamma_i(2\mathbf{k} + \mathbf{q})$. To measure a response function we must see how some physical quantity responds to such a phase twist. For this we measure the standard particle current. This leads us to the generating functional:

$$\mathcal{Z}[\mathbf{f}, \mathbf{g}] = \int \mathcal{D}(\bar{\psi}, \psi) \exp(iS[\bar{\psi}, \psi] + iS_j[\bar{\psi}, \psi]), \quad (1.19)$$

$$S_j[\bar{\psi}, \psi] = \sum_{\mathbf{k}, \mathbf{q}} \bar{\Psi}_{\mathbf{k}+\mathbf{q}}^T \begin{pmatrix} g_i(\mathbf{q}) & f_i(\mathbf{q}) + g_i(\mathbf{q}) \\ f_i(\mathbf{q}) - g_i(\mathbf{q}) & -g_i(\mathbf{q}) \end{pmatrix} \Psi_{\mathbf{k}} \gamma_i(2\mathbf{k} + \mathbf{q}),$$

where $\Psi^T = (\psi_C \ \psi_Q)$ and $S[\bar{\psi}, \psi]$ is the Schwinger-Keldysh action, e.g., Eq. (1.8)². The source field \mathbf{f} corresponds to the phase twist, and couples to the quantum current. The field \mathbf{g} couples to the observable particle current; the strange form in Keldysh space occurs in order to calculate normal-ordered expectations from the Schwinger-Keldysh path integral³. Taking derivatives with respect to these fields we find the current-current correlation function:

$$\chi_{ij}(\mathbf{q}, \omega = 0) = -\frac{i}{2} \frac{d^2 \mathcal{Z}[\mathbf{f}, \mathbf{g}]}{df_i(\mathbf{q}) dg_j(-\mathbf{q})} \Big|_{\mathbf{f}, \mathbf{g} \rightarrow 0}. \quad (1.20)$$

At this stage the calculation is exact; however, evaluating this requires the ability to calculate the partition function exactly, taking for the bare action an expression such as Eq. (1.8). If a linearised approach is valid, one can proceed by evaluating the path integral via a saddle point approach, first minimising over $\bar{\psi}, \psi$, and then including quadratic fluctuations about this saddle point. For an equilibrium system to respect sum rules, it is necessary that the saddle point should be calculated *in the presence of the fields \mathbf{f}, \mathbf{g}* . Repeating this in the non-equilibrium case leads to a generating function of the form $\mathcal{Z} \propto \exp(iS_0[\mathbf{f}, \mathbf{g}] - \text{Tr} \ln(1 + DA[\mathbf{f}, \mathbf{g}]))$, with contributions of the source terms to both the saddle point action and the action for fluctuations. Calculating the response function gives a sequence of terms that can be represented by the Feynman diagrams shown in Fig. 1.3. The first of these diagrams corresponds to the contribution from the saddle point action S_0 , the others arise from terms such as $\text{Tr}[D(d^2 A/df_i dg_j)]$ and $\text{Tr}[D(dA/df_i)D(dA/dg_j)]$.

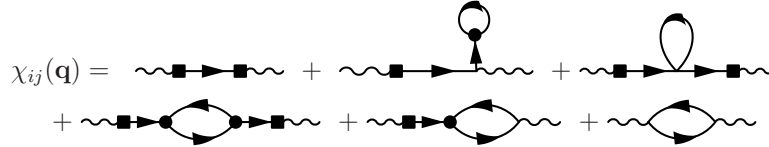


Figure 1.3 Feynman diagrams representing contributions to the response function at one-loop order. Solid circles and squares involve factors of the quasicondensate density, and wavy lines represent coupling to currents. The first five terms all contribute to the superfluid component, and the last gives the normal density. (Figure from Ref. [55].)

While the full expression coming from these diagrams [55] is rather involved, two simple conclusions can be drawn without reference to these details. The most important conclusion stemming from the above formalism is that (as long as the linearised theory is valid), a superfluid fraction will

exist, due to the form of the first five diagrams shown in Fig. 1.3. Crucially, each of these diagrams involves a term in which a single line carries the entire incoming and outgoing momentum, and so they give expressions of the form:

$$\chi_{ij}^{SF}(\mathbf{q}, \omega) \propto -|\psi_0|^2 q_i q_j D^R(\mathbf{q}, \omega),$$

where $D^R(\mathbf{q}, \omega)$ is the full retarded Green's function (including the normal and anomalous self energies arising due to the interaction terms in Eq. (1.8)). This structure reflects the fact that each diagram contains current vertices with one line having zero momentum, while the other carries the full momentum \mathbf{q} . Hence each diagram includes a factor $\gamma_i(\mathbf{q}) \propto q_i$. The retarded Green's function has poles corresponding to the normal mode frequencies given in Eq. (1.6). One may in fact show from the Keldysh action that the Green's function has the form $D^R(\mathbf{q}, \omega) \propto C/[\omega(\omega + i\gamma_{\text{net}}) - \xi_{\mathbf{q}}^2]$, which has the crucial feature that $D^R(\mathbf{q} \rightarrow 0, \omega = 0) \propto 1/q^2$. This feature (along with the structure of the diagrams) ensures a superfluid contribution to the response function.

The second important conclusion comes from the contribution of the last diagram, giving the normal fraction. This gives an expression:

$$m\chi_T = -\frac{i}{4} \int \frac{d\omega}{2\pi} \iint \frac{d^d k}{(2\pi)^d} \epsilon_k \text{Tr} [\sigma_z D_{\mathbf{k}}^K \sigma_z (D_{\mathbf{k}}^R + D_{\mathbf{k}}^A)],$$

which can be evaluated, and shown not to vanish unless the loss terms vanish. This has a simple physical interpretation: the noise associated with pumping and dissipation leads to the excitation of quasiparticles, and thus the creation of a normal fraction in all cases.

1.5.1 Experimental probes of superfluidity

As emphasised in the preceding sections, the superfluid density calculated above is a measure of the difference in how a system responds to transverse (rotational) vs longitudinal forces. As such, measurement of this superfluid response requires measuring the response to a rotational perturbation of some kind. For superfluid Helium, the classic experiment is that of Andronikashvili, using a torsional oscillator formed of parallel discs, and studying the changing inertia of the fluid as the temperature varies.

For polaritons, several issues arise: the particles are quasiparticles, which do not strongly couple to a rotating inertial frame, they live inside a semiconductor, and so applying a stirring force is challenging, and their rotation does not provide any measurable contribution to the mechanical angular

momentum. What is therefore required is a way to engineer an effective rotating frame *as seen by the polaritons*, and to measure the response of the polaritons to this.

Engineering a rotating frame for polaritons can be achieved in the same spirit as proposed for cold atoms [56, 57], namely manufacturing a real space Berry curvature arising from spatially varying spin structure of polariton eigenstates. The essence of such a synthetic rotation is to use the two-component spinor structure of the polariton to construct a spatially varying ground state $|\chi(\mathbf{r})\rangle$ such that the Berry connection $\mathbf{A}(\mathbf{r}) = i\langle\chi|\nabla\chi\rangle$ takes the form $\mathbf{A}(\mathbf{r}) = m\omega(r)\hat{\mathbf{z}} \times \mathbf{r}$, corresponding to a synthetic rotating frame. Such a configuration arises from the ground state of the spin Hamiltonian $H = \lambda[\ell_0^2\sigma^z + r^2(e^{2i\theta}\sigma^- + \text{H.c.})]$, where r, θ are in-plane polar coordinates, and σ^i are Pauli matrices for the spinor basis. The term $\lambda\ell_0^2\sigma^z$ corresponds to a Zeeman splitting induced by an external field. The other term requires either an induced strain, a strong radial magnetic field (i.e. diverging in the plane of the polariton system). This leads to an angular velocity peaking at $\omega \simeq 0.3\hbar/m\ell_0^2$ around $r \sim \ell_0$.

Measuring the response to such a field is in principle possible in a variety of ways, since an advantage of the polariton system is the ability to directly probe polariton correlation functions in both real and momentum space. In particular, it is in principle possible to measure correlations such as $\langle a_{\mathbf{k}+\mathbf{q}}^\dagger a_{\mathbf{k}} \rangle$ as a function of \mathbf{k}, \mathbf{q} by taking the interference between two momentum-space images of the condensate, displaced in real space, with a variable phase delay, i.e. calculating $I(\phi_d) = \langle (a_{\mathbf{k}}^\dagger + e^{-i\phi_d}a_{\mathbf{k}+\mathbf{q}}^\dagger)(a_{\mathbf{k}} + e^{i\phi_d}a_{\mathbf{k}+\mathbf{q}}) \rangle$, and mapping the fringe visibility as one varies ϕ_d . Real space displaced fringe visibility maps are routinely measured, see e.g. [58]; the equivalent momentum space tomography would allow access to the current induced by a given force, and thus reconstruction of the response function $\chi_{ij}(\mathbf{q})$.

Existing experiments probing aspects of superfluidity in polaritons are still far from this limit. Indeed what has been observed thus far is suppression of drag, rather than the difference between transverse and longitudinal response. In addition, such experiments to date have included measurements of the suppression of scattering from defects, as a function of velocity and intensity of a coherently driven condensate [59, 60].

1.6 Vortices and metastable flow in a driven dissipative system

As discussed in Section 1.2, the appearance of quantised vortices demonstrates the existence of short range coherence in a system, and is closely related to metastable persistent flow in a non-simply-connected geometry. We review here how these features are modified in a dissipative condensate. It is notable that the structure of vortices changes in the presence of drive and dissipation. Because the dissipation depends on density, the “continuity” equation derived from Eq. (1.4) takes the form:

$$\partial_t \rho + \nabla \cdot \mathbf{j} = (\gamma - \kappa - \Gamma \rho) \rho, \quad \mathbf{j} \equiv -\frac{i}{2m} (\varphi^* \nabla \varphi - \varphi \nabla \varphi^*). \quad (1.21)$$

This has the consequence that near the core of a vortex, where density is depleted, there is net gain, and so there must be a current with non-vanishing divergence. Given that current can be rewritten as $\mathbf{j} = \frac{\rho}{m} \nabla [\arg(\varphi)]$, this diverging current implies that vortices in a driven dissipative system must have a spiral structure, with radial as well as angular variation of phase. Such spiral vortices have been discussed in the context of nonlinear optics [61]. The existence of a spiral structure can modify the force between a pair of vortices, and so may modify the nature of the vortex binding/unbinding at the KT transition. This provides a further complication — in addition to that provided by the strong nonlinearity of the KPZ equation — in understanding the KT transition in a driven dissipative system.

There can also be cases in which combinations of spatial variation of drive, dissipation, and potential trapping destabilise the vortex free configuration, and instead stabilise configurations such as vortex lattices [62, 63]. However, understanding whether such configurations occur in practice requires analysis of the normal state, going beyond the scope of the complex GPE [5].

Because of the photon component of a polariton condensate, it is also possible to directly imprint vortices on the condensate, by using a coherent Gauss-Laguerre beam. Calculations using stochastic classical field methods have shown [64] how such pulses can create metastable vortex states in both simply and non-simply-connected geometries. The additional noise associated with pumping and decay means that the timescale for a vortex to move out of such a condensate can be relatively short: rather than quantum tunnelling, it can diffuse across a small annulus, driven by noise from the pump and decay terms.

Vortices have been clearly observed in polariton condensates [58], however since most images of polariton condensates require long integration times, vortices can only be seen if they are either stationary (pinned on dis-

order), or if they move along a repeatable path [65] (so that averages over many realisations recover the same trajectory). As such, indirect methods of imaging vortices may be necessary, such as interference measurements with angular offsets [64], or, for vortex lattices, energy resolved and interference images [63].

1.7 Future directions, open questions

The most profound open question is how the KPZ roughening interacts with the fact that phase is a compact variable and can thus support topological defects. As discussed previously two scenarios seem possible. It may be that as the KPZ equation flows to strong nonlinearity, the destruction of algebraic order also destroys any resistance to vortex proliferation. In this case, correlations are always exponential, there is no ordered phase, no superfluidity, and no phase transition. In this scenario, all experiments on polariton condensates would be finite size effects, although potentially exceptionally large system sizes needed before the “true” behaviour becomes visible. The other possible scenario is that the strong nonlinearity is compatible with vortex binding. In this case, there would be a phase transition between a high temperature phase showing exponential decay of correlations, and a low temperature phase with stretched exponential decay. If this scenario holds then despite the absence of algebraic order, there can be a non-zero superfluid stiffness [53]. If such a phase transition exists, it could potentially require a new universality class, distinct from the equilibrium KT universality class.

While the above questions concern the fundamental physics of the thermodynamic limit, a second set of questions concern the signatures of this behaviour visible in finite experimental systems. Physical [29, 50] and numerical [51] experiments have observed power law correlations, but with surprising values of the power law exponent; understanding the physical origin of this behaviour may help understand the nature of the driven dissipative system. Finally, experiments directly probing the superfluid response function — i.e. measuring the superfluid fraction — of a driven dissipative condensate have yet to be realised. Even in the context of cold atom systems, direct measurements of the superfluid fraction remain challenging [56]. Realising such measurements for driven dissipative systems can provide confirmation and guidance to the theoretical question of whether superfluidity exists in these systems, and whether it is a finite-size or thermodynamic phenomenon.

Notes

- 1 More precisely, the perturbation theory is valid when a suitable dimensionless measure of the ratio of the non-linear $\lambda_{x,y}$ terms in the KPZ equation to the linear ones is small; this measure proves to be the parameter g defined below.
- 2 In Ref. [55] a different model action was taken, involving frequency dependent gain. This difference does not affect the general points discussed below, but does affect several details of the calculation.
- 3 One can alternatively use a simpler form at the expense of introducing causality factors to ensure normal ordering.

References

- [1] Huang, Kerson. 1995. Bose-Einstein Condensation and Superfluidity. Page 31 of: Griffin, A, Snoke, D, and Stringari, S (eds), *Bose-Einstein Condens.* Cambridge: Cambridge University Press.
- [2] Leggett, A. J. 1999. Superfluidity. *Rev. Mod. Phys.*, **68**61(99), 318–323.
- [3] Hohenberg, P.C., and Martin, P.C. 2000. Microscopic Theory of Superfluid Helium. *Ann. Phys. (N. Y.)*, **281**(1-2), 636–705.
- [4] Leggett, A J. 2006. *Quantum Liquids: Bose Condensation and Cooper Pairing in Condensed-Matter Systems*. Oxford University Press.
- [5] Carusotto, Iacopo, and Ciuti, Cristiano. 2013. Quantum fluids of light. *Rev. Mod. Phys.*, **85**(1), 299.
- [6] Klaers, Jan, Schmitt, Julian, Vewinger, Frank, and Weitz, Martin. 2010. Bose-Einstein condensation of photons in an optical microcavity. *Nature*, **468**(7323), 545–8.
- [7] Demokritov, S O, Demidov, V E, Dzyapko, O, Melkov, G A, Serga, A A, Hillebrands, B, and Slavin, A N. 2006. Bose-Einstein condensation of quasi-equilibrium magnons at room temperature under pumping. *Nature*, **443**(7110), 430–3.
- [8] Falkenau, Markus, Volchkov, Valentin V., Rührig, Jahn, Griesmaier, Axel, and Pfau, Tilman. 2011. Continuous Loading of a Conservative Potential Trap from an Atomic Beam. *Phys. Rev. Lett.*, **106**(16), 163002.
- [9] Mewes, M.-O., Andrews, M. R., Kurn, D. M., Durfee, D. S., Townsend, C. G., and Ketterle, W. 1997. Output Coupler for Bose-Einstein Condensed Atoms. *Phys. Rev. Lett.*, **78**(Jan), 582–585.
- [10] Robins, N. P., Figl, C., Jeppesen, M., Dennis, G. R., and Close, J. D. 2008. A pumped atom laser. *Nat. Phys.*, **4**, 731.
- [11] Robins, N. P., Altin, P. A., Debs, J. E., and Close, J. D. 2013. Atom lasers: Production, properties and prospects for precision inertial measurement. *Physics Reports*, **529**, 265296.
- [12] Yang, C. N. 1962. Concept of Off-Diagonal Long-Range Order and the Quantum Phases of Liquid He and of Superconductors. *Rev. Mod. Phys.*, **34**(4), 694–704.
- [13] Pitaevskii, Lev. P, and Stringari, Sandro. 2003. *Bose-Einstein Condensation*. Oxford: Clarendon Press.
- [14] Hess, G B, and Fairbank, W M. 1967. Measurements of Angular Momentum in Superfluid Helium. *Phys. Rev. Lett.*, **19**, 216–218.
- [15] Griffin, Allan. 1994. *Excitations in a Bose-condensed Liquid*. Cambridge: Cambridge University Press.

- [16] Mermin, N D, and Wagner, H. 1966. Absence of Ferromagnetism or Antiferromagnetism in One- or Two- Dimensional Isotropic Heisenberg Models. *Phys. Rev. Lett.*, **17**, 1133.
- [17] Kosterlitz, JM, and Thouless, DJ. 1973. Ordering, metastability and phase transitions in two-dimensional systems. *J. Phys. C Solid State Phys.*, **6**, 1181.
- [18] Kosterlitz, J M. 1974. The critical properties of the two-dimensional XY model. *J. Phys. C Solid State Phys.*, **7**(6), 1046–1060.
- [19] Berezinskii, VL. 1972. Destruction of long-range order in one-dimensional and two-dimensional systems possessing a continuous symmetry group. ii. quantum systems. *J. Exp. Theor. Phys.*, **34**(3).
- [20] Nelson, David R. 1977. Universal Jump in the Superfluid Density of Two-Dimensional Superfluids. *Phys. Rev. Lett.*, **39**(19), 1201–1205.
- [21] Chaikin, P M, and Lubensky, T C. 1995. *Principles of Condensed Matter Physics*. Cambridge, UK: Cambridge University Press.
- [22] Wouters, M, and Carusotto, I. 2006. Absence of long-range coherence in the parametric emission of photonic wires. *Phys. Rev. B*, **74**(24), 1–6.
- [23] Szymańska, M H, Keeling, J., and Littlewood, P. B. 2006. Nonequilibrium Quantum Condensation in an Incoherently Pumped Dissipative System. *Phys. Rev. Lett.*, **96**(23), 230602.
- [24] Szymańska, M. H., Keeling, J., and Littlewood, P. 2007. Mean-field theory and fluctuation spectrum of a pumped decaying Bose-Fermi system across the quantum condensation transition. *Phys. Rev. B*, **75**(19), 195331.
- [25] Aranson, Igor, and Kramer, Lorenz. 2002. The world of the complex Ginzburg-Landau equation. *Rev. Mod. Phys.*, **74**(1), 99–143.
- [26] Astrakharchik, G. E., and Pitaevskii, L. P. 2004. Motion of a heavy impurity through a Bose-Einstein condensate. *Phys. Rev. A*, **70**(Jul), 013608.
- [27] Wouters, Michiel, and Carusotto, Iacopo. 2010. Superfluidity and Critical Velocities in Nonequilibrium Bose-Einstein Condensates. *Phys. Rev. Lett.*, **105**(2), 20602.
- [28] Cancellieri, E., Marchetti, F M, Szymańska, M. H., and Tejedor, C. 2010. Superflow of resonantly driven polaritons against a defect. *Phys. Rev. B*, **82**(22), 224512.
- [29] Roumpos, Georgios, Lohse, Michael, Nitsche, Wolfgang H., Keeling, Jonathan, Szymańska, Marzena Hanna, Littlewood, Peter B., Löffler, Andreas, Höfling, Sven, Worschech, Lukas, Forchel, Alfred, and Yamamoto, Yoshihisa. 2012. Power-law decay of the spatial correlation function in exciton-polariton condensates. *Proc. Nat. Acad. Sci.*, **109**(17), 6467.
- [30] Chiocchetta, Alessio, and Carusotto, Iacopo. 2013. Non-equilibrium quasi-condensates in reduced dimensions. *Eur. Phys. Lett.*, **102**(6), 67007.
- [31] Kamenev, Alex. 2011. *Field Theory of Non-Equilibrium Systems*. Cambridge: Cambridge University Press.
- [32] Graham, R, and Tel, T. 1990. Steady-state ensemble for the complex Ginzburg-Landau equation with weak noise. *Phys. Rev. A*, **42**(8).
- [33] Sieberer, L. M., Huber, S. D., Altman, E, and Diehl, S. 2014. Nonequilibrium functional renormalization for driven-dissipative Bose-Einstein condensation. *Phys. Rev. B*, **89**(13), 134310.
- [34] Sieberer, L M, Huber, S D, Altman, E, and Diehl, S. 2013. Dynamical Critical Phenomena in Driven-Dissipative Systems. *Phys. Rev. Lett.*, **110**(19), 195301.

- [35] Täuber, Uwe C., and Diehl, Sebastian. 2014. Perturbative Field-Theoretical Renormalization Group Approach to Driven-Dissipative Bose-Einstein Criticality. *Phys. Rev. X*, **4**(2), 021010.
- [36] Altman, Ehud, Sieberer, Lukas M., Chen, Leiming, Diehl, Sebastian, and Toner, John. 2015. Two-Dimensional Superfluidity of Exciton Polaritons Requires Strong Anisotropy. *Phys. Rev. X*, **5**(Feb), 011017.
- [37] Kardar, Mehran, Parisi, Giorgio, and Zhang, Yi-Cheng. 1986. Dynamic Scaling of Growing Interfaces. *Phys. Rev. Lett.*, **56**(Mar), 889–892.
- [38] Chen, Leiming, and Toner, John. 2013. Universality for Moving Stripes: A Hydrodynamic Theory of Polar Active Smectics. *Phys. Rev. Lett.*, **111**(8), 088701.
- [39] Wolf, DE. 1991. Kinetic roughening of vicinal surfaces. *Phys. Rev. Lett.*, **67**(13), 1783–1786.
- [40] Kim, Jin, and Kosterlitz, J. 1989. Growth in a restricted solid-on-solid model. *Phys. Rev. Lett.*, **62**(19), 2289–2292.
- [41] Miranda, Vladimir G., and Aarão Reis, Fábio D. A. 2008. Numerical study of the Kardar-Parisi-Zhang equation. *Phys. Rev. E*, **77**(3), 031134.
- [42] Marinari, Enzo, Pagnani, Andrea, and Parisi, Giorgio. 2000. Critical exponents of the KPZ equation via multi-surface coding numerical simulations. *J. Phys. A: Math. Gen.*, **33**(46), 8181–8192.
- [43] Ghaisas, S. 2006. Stochastic model in the Kardar-Parisi-Zhang universality class with minimal finite size effects. *Phys. Rev. E*, **73**(2), 022601.
- [44] Chin, Chen-Shan, and den Nijs, Marcel. 1999. Stationary-state skewness in two-dimensional Kardar-Parisi-Zhang type growth. *Phys. Rev. E*, **59**(3), 2633–2641.
- [45] Tang, Lei-Han, Forrest, Bruce, and Wolf, Dietrich. 1992. Kinetic surface roughening. II. Hypercube-stacking models. *Phys. Rev. A*, **45**(10), 7162–7179.
- [46] Fisher, Matthew P. A., and Grinstein, G. 1992. Nonlinear transport and $1/f^\alpha$ noise in insulators. *Phys. Rev. Lett.*, **69**(Oct), 2322–2325.
- [47] Gladilin, Vladimir N, Ji, Kai, and Wouters, Michiel. 2014. Spatial coherence of weakly interacting one-dimensional nonequilibrium bosonic quantum fluids. *Phys. Rev. A*, **90**(2), 023615.
- [48] Ji, Kai, Gladilin, Vladimir N., and Wouters, Michiel. 2015. Temporal coherence of one-dimensional nonequilibrium quantum fluids. *Phys. Rev. B*, **91**(Jan), 045301.
- [49] He, Liang, Sieberer, Lukas M, Altman, Ehud, and Diehl, Sebastian. 2014. *Scaling properties of one-dimensional driven-dissipative condensates*.
- [50] Nitsche, Wolfgang H., Kim, Na Young, Roumpos, Georgios, Schneider, Christian, Kamp, Martin, Höfling, Sven, Forchel, Alfred, and Yamamoto, Yoshihisa. 2014. Algebraic order and the Berezinskii-Kosterlitz-Thouless transition in an exciton-polariton gas. *Phys. Rev. B*, **90**(Nov), 205430.
- [51] Dagvadorj, G., Fellows, J. M., Matyjaskiewicz, S., Marchetti, F. M., Carusotto, I., and Szymańska, M. H. 2014. *Non-equilibrium Berezinskii-Kosterlitz-Thouless Transition in a Driven Open Quantum System*.
- [52] Shelykh, I A, Kavokin, A V, Rubo, Yuri G, Liew, T C H, and Malpuech, G. 2010. Polariton polarization-sensitive phenomena in planar semiconductor microcavities. *Semiconductor Science and Technology*, **25**(1), 013001.
- [53] Sieberer, Lukas M, and Diehl, Sebastian. 2015. Superfluidity of a Driven-Dissipative System.

- [54] Janot, Alexander, Hyart, Timo, Eastham, Paul, and Rosenow, Bernd. 2013. Superfluid Stiffness of a Driven Dissipative Condensate with Disorder. *Phys. Rev. Lett.*, **111**(23), 230403.
- [55] Keeling, Jonathan. 2011. Superfluid Density of an Open Dissipative Condensate. *Phys. Rev. Lett.*, **107**(8), 080402.
- [56] Cooper, Nigel R., and Hadzibabic, Zoran. 2010. Measuring the Superfluid Fraction of an Ultracold Atomic Gas. *Phys. Rev. Lett.*, **104**(3), 030401.
- [57] John, Sebastian T, Hadzibabic, Zoran, and Cooper, Nigel R. 2011. Spectroscopic method to measure the superfluid fraction of an ultracold atomic gas. *Phys. Rev. A*, **83**(2), 023610.
- [58] Lagoudakis, K. G., Wouters, M., Richard, M., Baas, A., Carusotto, I., André, R., Dang, Le Si, and Deveaud-Plédran, B. 2008. Quantized vortices in an exciton-polariton condensate. *Nat. Phys.*, **4**(9), 706–710.
- [59] Amo, A, Sanvitto, D, Laussy, F P, Ballarini, D, del Valle, E, Martin, M D, Lemaître, A, Bloch, J, Krizhanovskii, D N, Skolnick, M S, Tejedor, C, and Viña, L. 2009a. Collective fluid dynamics of a polariton condensate in a semiconductor microcavity. *Nature*, **457**(7227), 291–5.
- [60] Amo, Alberto, Lefrère, Jérôme, Pigeon, Simon, Adrados, Claire, Ciuti, Cristiano, Carusotto, Iacopo, Houdré, Romuald, Giacobino, Elisabeth, and Bramati, Alberto. 2009b. Superfluidity of polaritons in semiconductor microcavities. *Nat. Phys.*, **5**(11), 805–810.
- [61] Staliunas, K, and Sanchez-Morcillo, V J. 2003. *Transverse Patterns in Non-linear Optical Resonators*. Berlin: Springer-Verlag.
- [62] Keeling, Jonathan, and Berloff, Natalia G. 2008. Spontaneous Rotating Vortex Lattices in a Pumped Decaying Condensate. *Phys. Rev. Lett.*, **100**(25), 250401.
- [63] Borgh, Magnus O., Keeling, Jonathan, and Berloff, Natalia G. 2010. Spatial pattern formation and polarization dynamics of a nonequilibrium spinor polariton condensate. *Phys. Rev. B*, **81**(23), 235302.
- [64] Wouters, Michiel, and Savona, Vincenzo. 2010. Superfluidity of a nonequilibrium Bose-Einstein condensate of polaritons. *Phys. Rev. B*, **81**(5), 054508.
- [65] Lagoudakis, K. G., Manni, F., Pietka, B., Wouters, M., Liew, T. C. H., Savona, V., Kavokin, A. V., André, R., and Deveaud-Plédran, B. 2011. Probing the Dynamics of Spontaneous Quantum Vortices in Polariton Superfluids. *Phys. Rev. Lett.*, **106**(11), 115301.